MEDICAL ROBOTICS

Robotic hand augmentation drives changes in neural body representation

Paulina Kieliba[1], Danielle Clode[1,2], Roni O. Maimon-Mor[1,3], Tamar R. Makin[1,4]*

Humans have long been fascinated by the opportunities afforded through augmentation. This vision not only depends on technological innovations but also critically relies on our brain's ability to learn, adapt, and interface with augmentation devices. Here, we investigated whether successful motor augmentation with an extra robotic thumb can be achieved and what its implications are on the neural representation and function of the biological hand. Able-bodied participants were trained to use an extra robotic thumb (called the Third Thumb) over 5 days, including both lab-based and unstructured daily use. We challenged participants to complete normally bimanual tasks using only the augmented hand and examined their ability to develop hand-robot interactions. Participants were tested on a variety of behavioral and brain imaging tests, designed to interrogate the augmented hand's representation before and after the training. Training improved Third Thumb motor control, dexterity, and hand-robot coordination, even when cognitive load was increased or when vision was occluded. It also resulted in increased sense of embodiment over the Third Thumb. Consequently, augmentation influenced key aspects of hand representation and motor control. Third Thumb usage weakened natural kinematic synergies of the biological hand. Furthermore, brain decoding revealed a mild collapse of the augmented hand's motor representation after training, even while the Third Thumb was not worn. Together, our findings demonstrate that motor augmentation can be readily achieved, with potential for flexible use, reduced cognitive reliance, and increased sense of embodiment. Yet, augmentation may incur changes to the biological hand representation. Such neurocognitive consequences are crucial for successful implementation of future augmentation technologies.

INTRODUCTION

Motor augmentation is a growing field aimed at extending our physical abilities. Engineers are currently developing extra robotic fingers, and even entire arms, to augment our bodies by expanding our natural motor repertoire (*1*–*6*). These augmentative devices aim to change the way we interact with the environment, which entails changes to how we move and operate our biological body. Yet, despite the rapid advancements in augmentative technologies, little notice is given to the crucial question of how the human brain might support them. Here, we investigate whether the human brain could accommodate motor control of an extra robotic finger, focusing on its impact on the neural representation of the biological hand.

The hand has a well-established functional representation in the brain, with each of the fingers represented relative to the others. This neural fingerprint of the hand develops very early on (*7*, *8*). It is highly consistent within (*9*) and across (*10*) participants and is preserved even after severe loss of motor functions due to, e.g., stroke (*10*), spinal cord injury (*11*), disability (*12*), or even hand amputation (*13*–*15*). Similarly, recent studies on motor learning in adults show that whereas premotor and parietal regions show reorganization of hand representation in the early stages (first week) of intensive motor training, hand representation in the primary motor cortex (M1) remains stable throughout training (*16*, *17*). At the same time, hand representation has been suggested to reflect daily hand use (*10*), with studies showing that it may be altered under constrained circumstances. In musicians' dystonia, a clinical condition involving increased finger enslavement after intensive practice of the skill, the individualized representation of single fingers has been shown to collapse (*18*). However, other research was unable to replicate this finding (*19*).

Here, we trained able-bodied people to use an extra robotic thumb [the Third Thumb, designed by Clode (*20*), hereafter "Thumb"] over the course of 5 days, including both lab-based and "in-the-wild," unstructured daily use. The Thumb is a supernumerary robotic finger, with two degrees of freedom, controlled by pressure exerted with the big toes, designed to extend the natural repertoire of hand movements (Movie 1; Fig. 1, A and B; and fig. S1). We

Movie 1. Overview of the study approach, training tasks, and key results. Using the Third Thumb, we examined how people's brains adapt while learning to use an extra robotic finger. We found that after 5 days of training, participants were able to integrate motor control of the Thumb with the movements of their natural hand, reporting increased sense of embodiment of the device. Yet, using the Thumb influenced participants' natural hand movements and hand representation in the brain.

[1]Institute of Cognitive Neuroscience, University College London, 17 Queen Square, London WC1N 3AZ, UK. [2]Dani Clode design, 40 Hillside Road, London SW2 3HW, UK. [3]WIN Centre, University of Oxford, Oxford OX3 9DU, UK. [4]Wellcome Trust Centre for Neuroimaging, University College London, London WC1N 3AR, UK.
*Corresponding author. Email: t.makin@ucl.ac.uk

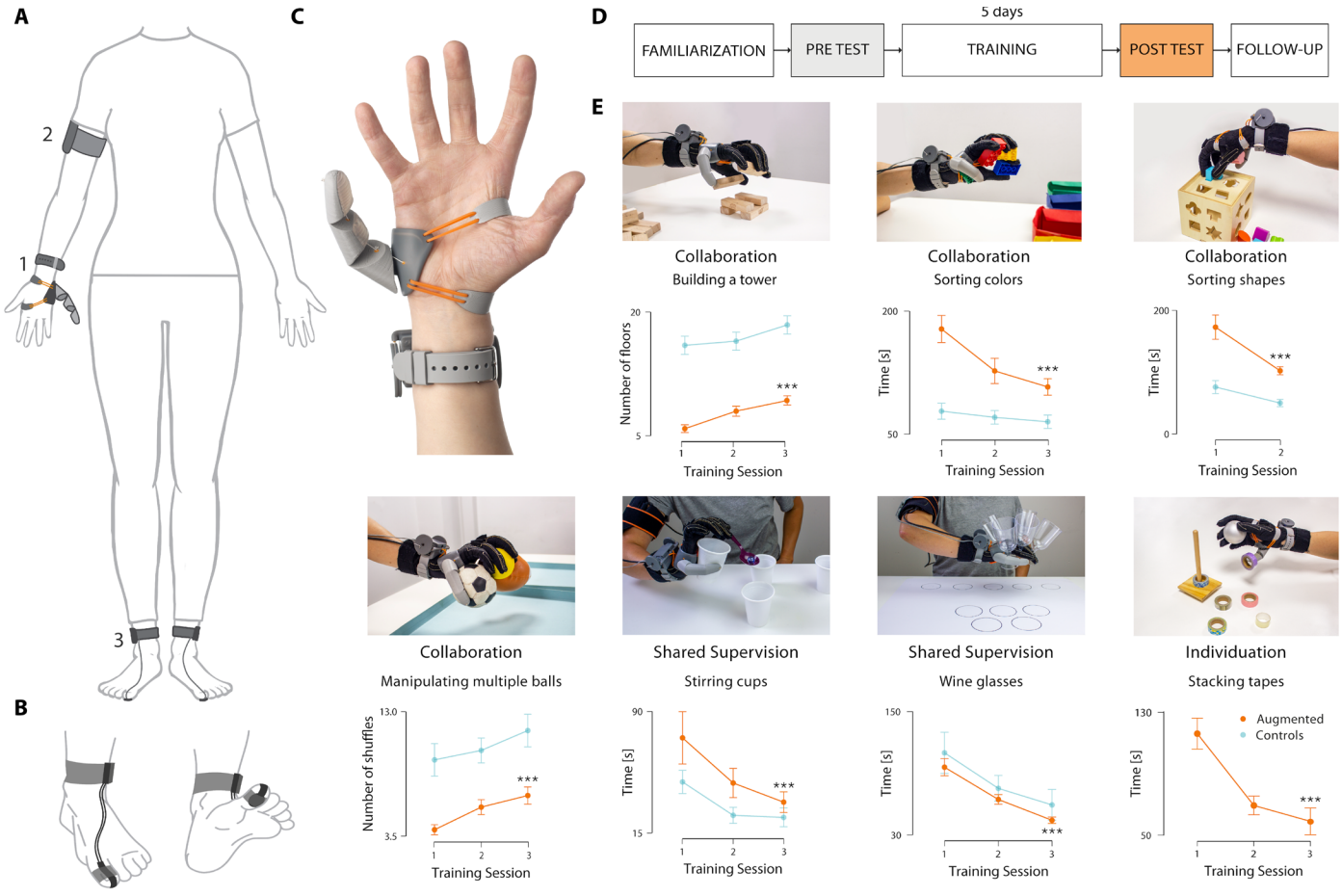

Fig. 1. Experimental design of the study. (**A** to **C**) The Third Thumb is a 3D-printed robotic thumb. Mounted on the side of the palm (1), the Thumb is actuated by two motors (fixed to a wrist band), allowing for independent control over flexion/adduction. The Thumb is powered by (2) an external battery, strapped around the arm and wirelessly controlled by (3) two force sensors fixed to the underside of the participant's big toes. (**D**) Experimental design for the augmentation group. (**E**) Examples of the in-lab training tasks used for hand-Thumb collaboration, shared supervision, and Thumb individuation. Augmentation participants showed significant performance improvements on all of the tasks across training sessions. The dots depict group means, and error bars indicate SEM. Asterisks denote significant effect of time at ***$P < 0.001$. See fig. S2 for statistical quantification of the improvements seen in the control group.

examined participants' ability to develop motor skill and dexterity with the Thumb under daily life settings, across key aspects of hand-robot interactions, such as collaboration, shared supervision, and individuation. During training, we also tracked (biological) finger co-use and compared it with normal hand use. We tested for changes in motor control and embodiment of the Thumb, as well as hand-Thumb coordination before and after training. Augmented participants were compared with a control group that underwent a similar training regime while wearing a static version of the Thumb. We also examined how neural hand and body representation changed after training. We hypothesized that successful hand-robot cooperation will promote changes to finger co-use and thus modify both biological and artificial body representation.

RESULTS

The Third Thumb

The Third Thumb is a three-dimensionally (3D) printed robotic thumb (*20*), originally designed as an augmentative, general-use tool for able-bodied people (see Movie 1). The Thumb is worn over the ulnar side of the right palm, opposite to the user's natural thumb (Fig. 1, A and B). It is actuated by two motors, allowing proportional control of two independent degrees of freedom, flexion/extension and adduction/abduction. The motors are mounted on a wrist strap (Fig. 1A, 1) and powered by an external battery pack worn on the upper arm (Fig. 1A, 2). The movement of the Thumb is controlled with pressure sensors fixed to the underside of the big toes of the user's feet (fig. S1). The pressure sensors are powered by the external batteries secured around each ankle (Fig. 1A, 3). A wireless communication protocol is used to send the signal from the pressure sensors to the motors that actuate the Thumb. Pressure exerted with the right toe pulls the Thumb across the hand (flexion), whereas the pressure exerted with the left toe pulls the Thumb up toward the fingers (adduction). The extent of Thumb movement is fully proportional to the pressure applied. Hence, the Thumb can be used when sitting or standing, but not while walking. The wireless design allows users to operate the Thumb in an unstructured environment, providing us with the unique opportunity to encourage participants to use the Thumb outside the lab and unsupervised.

Daily training improves hand-Thumb coordination, even with reduced visual information and increased cognitive load

We first characterized the motor performance of the augmented hand throughout the 5 days of Thumb usage. Augmentation participants completed five daily in-lab training sessions (1.58 ± 0.22 hours; mean ± SD) and were additionally encouraged to use the Thumb outside the lab in unstructured environment (2.61 ± 1.18 hours; self-reported). The average use time, as quantified by the automatic usage logs, was 2.95 ± 0.84 hours/day, out of which a total of 1.37 ± 0.49 hours involved active Thumb movement.

During daily training sessions, participants were presented with a variety of reaching, grasping, and in-hand manipulation tasks designed to introduce complex hand-robot interactions and to be purposefully challenging to perform with only one hand (see movie S1). In the collaboration tasks, participants had to use the Thumb together with another finger to pick up multiple objects. In the shared supervision tasks, participants had to use the Thumb to extend the natural grip of the hand and to free up the use of their biological fingers. Last, in the individuation task, participants had to work on the fine motor control of the Thumb while having their hand fully occupied with a task-irrelevant object. Augmentation participants showed significant improvement on all the training tasks (main effect of time for all tasks: $P < 0.001$, $\eta_p^2 > 0.5$; Fig. 1D).

Motor control was further assessed using a hand-Thumb coordination task, requiring participants to oppose the Thumb to their biological fingertips. Although controlling the Thumb with the big toes may seem unusual, participants were able to successfully perform the hand-Thumb coordination task even at baseline (Fig. 2B), although this performance was significantly improved after training. Significant improvements were observed both during daily training [$F(4,76) = 28.24$, $P < 0.001$, $\eta_p^2 = 0.6$; Fig. 2, A to C) and when comparing the performance before and after the 5 days of training, using a sequential variation of the same task (see Materials and Methods). Here, augmentation participants showed significant improvements, not only with vision [$t(19) = 8.96$, $P < 0.001$, $\eta_p^2 = 0.81$] but also when blindfolded [$t(19) = 7.40$, $P < 0.001$, $\eta_p^2 = 0.74$; Fig. 2E], indicating improved Thumb proprioception.

Because the improvements described above could be skewed due to task repetition, we also tested a group of 11 control participants who underwent similar pre- and posttests and training regime but wore a static version of the Thumb for the same duration of time, 4.11 ± 1.06 hours/day [$t(29) = 0.526$, $P = 0.6$, Bayesian factor (BF) = 0.39], out of which 2.93 ± 1.34 hours were outside of the lab [$t(29) = -0.697$, $P = 0.49$, BF = 0.42 for wear-time group comparison]. Similar to the augmentation group, the control group, who had to develop five-fingered solutions to the same problems, showed proportional improvements in nearly all training tasks (fig. S2). Because control participants did not have to learn to control the robotic device, their training performance was significantly better as compared with the augmentation group, with the exception of the shared supervision tasks. This indicates that given specific task demands, the extended motor ability provided by the Thumb can also increase participants' functional efficiency. The control group was only allowed to use the Thumb during the pre-post sequential hand-Thumb coordination test. Although control participants showed significant pre-post improvements [with vision: $t(9) = 3.74$, $P = 0.005$; without vision: $t(9) = 2.35$, $P = 0.043$], those were significantly lower than the ones observed in the augmentation group, both with vision [significant effect of the group revealed by analysis of covariance (ANCOVA); $F(1,27) = 22.86$, $P < 0.001$, $\eta_p^2 = 0.44$] and blindfolded [$F(1,27) = 11.96$, $P = 0.002$, $\eta_p^2 = 0.28$].

A key component for successful augmentation is being able to multitask, even when not paying attention to controlling the device. Augmentation participants' motor performance with the Thumb was not influenced by increased cognitive load. This was examined during the first and last days of training, using a dual task (*21*, *22*), requiring participants to perform simple arithmetic operations while simultaneously using the Thumb to complete a collaboration task (building a tower). We found no significant cognitive load × session interaction [$F(1,16) = 0.003$, $P = 0.959$, BF = 0.34] and no main effect of cognitive load [$F(1,16) = 2.465$, $P = 0.136$, BF = 0.32; Fig. 2D] on the motor performance. At the same time, participants made a modest number of arithmetic mistakes (on average, 15 to 19% of trials per participant), showing that the dual task indeed increased the cognitive load demands.

Together, these results indicate that participants learned to operate the Thumb under a variety of circumstances, extending beyond their specific training, and performed similarly with and without the increased cognitive load. Yet, with the exception of the shared supervision tasks, training performance of the augmentation group was reduced relative to controls, highlighting that extensive, long-term practice is needed to functionally benefit from motor augmentation.

Training enhances subjective sense of Thumb embodiment

We also assessed the perceived (phenomenological) sense of embodiment of the Thumb after the training period, relative to baseline. During pre- and posttest sessions, participants were asked to respond to statements relating to key embodiment features (*23*, *24*). Augmentation participants reported a significant increase of embodiment in each of the four categories [body ownership: $t(13) = 6.57$, $P < 0.001$, $\eta_p^2 = 0.77$; agency: $t(13) = 4.07$, $P < 0.001$, $\eta_p^2 = 0.56$; body image: $t(13) = 5.215$, $P < 0.001$, $\eta_p^2 = 0.68$; somatosensation: $t(13) = 6.032$, $P < 0.001$, $\eta_p^2 = 0.74$; Fig. 2F]. The increased embodiment found in the augmentation group significantly exceeded that reported in the control group [agency: $F(1,21) = 10.013$, $P = 0.009$, $\eta_p^2 = 0.285$; body image: $F(1,21) = 11.16$, $P = 0.012$, $\eta_p^2 = 0.26$; body ownership: $F(1,21) = 4.07$, $P = 0.057$, $\eta_p^2 = 0.16$]. These results indicate that active usage is critical for developing proprioception and embodiment of the robotic Thumb. For the perceived somatosensation scores, the group comparison was nonsignificant (BF = 0.48).

Next, we examined potential changes to body image [perceptions and attitudes concerning one's body representation (*25*)]. Those were tested while participants were not wearing the Thumb. We found no significant pre- to post-changes in tactile judgments [$t(18) = 0.164$, $P = 0.87$, BF = 0.24]. Similarly, we did not observe any convincing evidence for visual judgment changes (see the Supplementary Materials) because our findings were not specific to the augmented hand [main effect of time: $F(1,16) = 6.89$, $P = 0.018$; hand × session interaction: $F(1,16) = 0.019$, $P = 0.89$, BF = 0.326]. Together, these findings indicate that although hand augmentation influences the sense of embodiment over the device, it does not necessarily influence one's own implicit body image.

Hand augmentation influences motor control of the natural hand

Next, we investigated the impact of hand augmentation on motor control of the augmented (right) hand. We first examined the

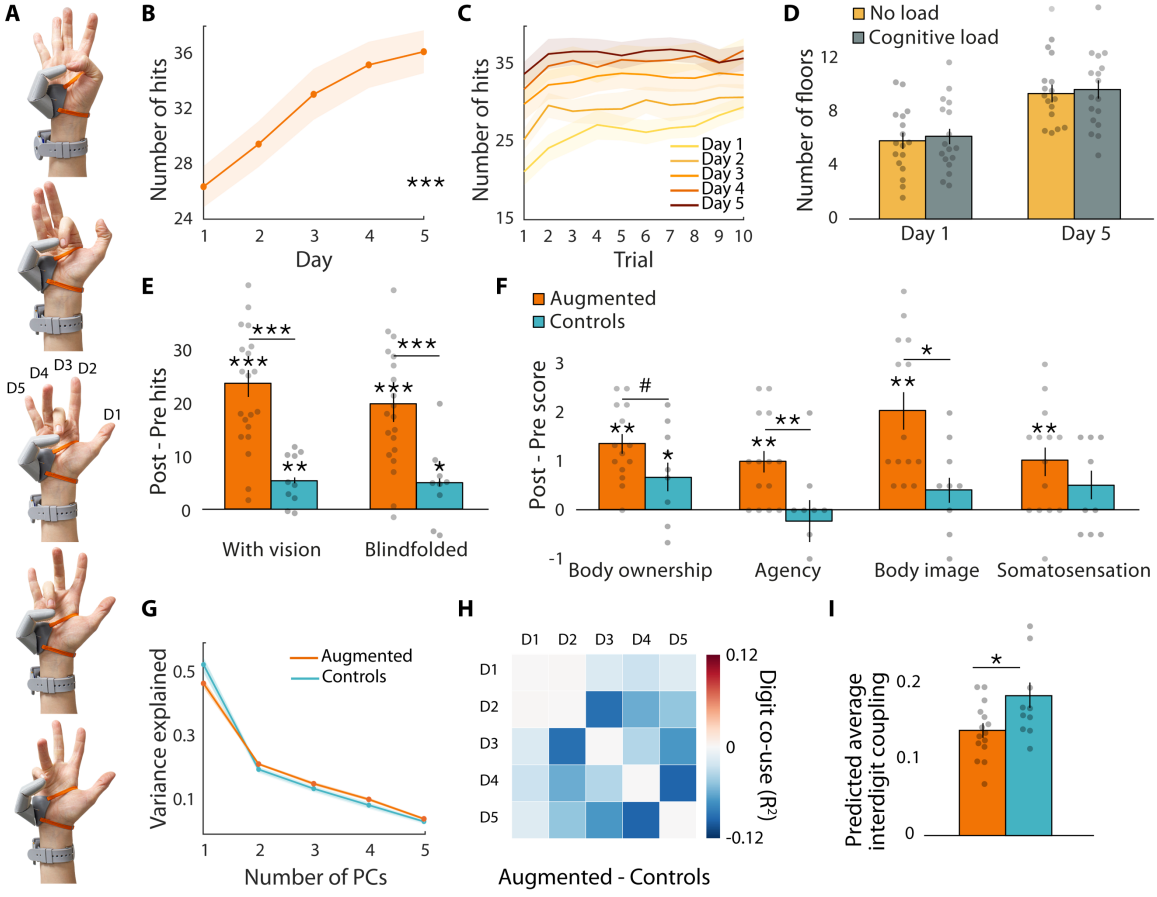

Fig. 2. Behavioral correlates of hand augmentation. (**A** to **C**) Augmentation participants showed significant daily improvement on the hand-Thumb coordination task. (**D**) Motor performance with the Thumb was not influenced by increased cognitive load during the first and last training days. (**E**) Augmentation participants showed greater improvement than controls on a hand-Thumb coordination task conducted before and after the training period. Participants showed improved performance even while blindfolded, indicating increased Thumb proprioception. (**F**) Self-reported Thumb embodiment increased significantly in the augmentation group after Thumb training. (**G**) Hand kinematics data collected during the training sessions. The first PC (synchronized movement across all five fingers) captured less variance in the augmentation group compared with controls, indicating less synchronized movements. (**H** and **I**) The augmentation group showed lower inter-finger coupling, relative to controls during Thumb use, indicating change to the natural finger coordination. The bars depict group means, and error bars represent SEM. Individual dots correspond to individual participants' average inter-finger (D1 to D5) coordination scores as predicted by the LMM (see Materials and Methods). Asterisks denote significant effects at $*P < 0.05$, $**P < 0.01$, and $***P < 0.001$.

complexity of the hand movements (i.e., kinematic synergies) captured with the CyberGlove during the in-lab training. We found that, in general, more principal components (PCs) were needed in the augmentation group, compared with the control group, to explain 80% of the total variance of the hand movements [$F(1,22) = 5.52$, $P = 0.03$, $\eta_p^2 = 0.2$; fig. S4B]. This difference was, however, strongly driven by the amount of variance explained by the first PC, corresponding to the coordinated flexion of all fingers (fig. S4A). The variance explained by this inter-finger synergy was significantly decreased in the augmentation group compared with controls [$F(1,22) = 6.27$, $P = 0.02$, $\eta_p^2 = 0.22$; Fig. 2G], whereas no difference was found between the first and the last days of training [$F(1,22) = 2.57$, $P = 0.12$, BF = 0.62]. Because the remaining PCs represent more intricate finger movements, the decrease of variance explained by the first kinematic synergy suggests more finger individuation in the augmentation group.

To uncover more detailed changes in biological finger coordination, we assessed the degree of kinematic coupling between individual digit pairs. Here again, no differences in finger coordination were found between the first and the last days of training [main effect of time: $F(1,23) = 1.3$, $P = 0.27$, BF = 0.17]. For the augmentation group, this finding indicates that the strategies implemented for incorporating the Thumb into the motor repertoire during day 1 were generally preserved throughout training. This is likely a consequence of our experimental design involving repeating the same set of tasks over multiple days. Consistent with the principal components analysis (PCA) results, we found significant differences in finger coordination implemented across groups [group × finger-pair interaction: $F(9,414) = 2.66$, $P = 0.005$], with an overall decrease in inter-finger coupling in the augmentation group relative to controls [main effect of group: $F(1,23) = 6.98$, $P = 0.01$; Fig. 2, H and I). Together, these results demonstrate small but robust changes to finger coordination, likely corresponding to more complex movement patterns acquired by the augmentation group during Thumb use.

Changes in inter-finger motor control were further investigated through force enslavement (involuntary force production by non-instructed fingers), measured before and after the training period. No significant group differences in force enslavement were found

[$F(1,27) = 0.06$, $P = 0.81$], with the results providing only anecdotal evidence for the increase of enslavement caused by the biological thumb in the augmentation group, post- compared with pretraining [$F(1,17) = 3.36$, $P = 0.08$; see fig. S5]. Given the ambiguous nature of these results, no clear conclusions could be drawn.

Biological hand's representation shrinks after Thumb use

Having observed altered finger coordination patterns in the augmentation group, as compared with controls, we sought to understand whether Thumb usage can influence the biological hand representation in the sensorimotor cortex. We used functional magnetic resonance imaging (fMRI) to compare neural hand representation before and after Thumb use, using the nonaugmented (left) hand as a within-participants control condition. During the scans, participants were required to make individuated finger movements with their biological fingers. Note that because of MRI safety considerations, participants were not wearing the Thumb during the scans.

To investigate changes to the augmented hand's representation, we estimated the dissimilarity between multivariate activity patterns elicited by individual fingers' movements in the sensorimotor cortex, as measured using cross-validated Mahalanobis distance (*26*). Small inter-finger distances indicate that the representation of the two fingers is more similar/overlapping, whereas larger distances imply more individuated finger representation. This experimental approach is the current gold standard in the field and has been extensively used to study plasticity and stability of hand representation (*9*, *10*, *13*, *14*).

Augmentation participants showed significantly reduced inter-finger distances of the augmented (right) hand's representation in the sensorimotor cortex after Thumb use [$t(25.1) = 2.3$, $P = 0.03$; Fig. 3]. In other words, the biological fingers became less distinctive from one another after training. This shrinkage effect was specific to the augmented hand, as demonstrated by a significant hand × time interaction [$F(1,722) = 12.89$, $P < 0.001$; Fig. 3C]. These findings show that using the extra Thumb not only alters the motor control of the biological hand but also influences how that hand is represented in the brain. Crucially, this effect was observed while participants were not using or even wearing the Thumb. A computational simulation, elaborated in Fig. 4, confirmed that the while results could be driven by both adaptive and maladaptive neural plasticity mechanisms.

We confirmed that the shrinkage of the augmented hand's representation was not associated with net differences in overall activity levels in the hand areas [hand × time interaction: $F(1,19) = 1.95$, $P = 0.18$, BF = 0.36] and that it did not influence the typicality of the representational structure [$t(19) = 1.12$, $P = 0.277$, BF = 0.4; see the Supplementary Materials]. No significant changes to the hand representation were observed in the control group, as demonstrated in both a pre-post comparison of the right hand's representational structure [$t(10.4) = -0.245$, $P = 0.81$, BF = 0.32] and the hand × time interaction [$F(1,342) = 0.71$, $P = 0.4$, BF = 0.95; see fig. S6]. This further indicates that without Thumb use, the biological hand's representation is relatively stable, as previously demonstrated in motor training studies (*16*, *17*). Note, however, that the three-way interaction (hand × time × group) did not reach significance [$F(1,1064) = 2.02$, $P = 0.16$], likely because of insufficient statistical power.

To further test whether the observed shrinkage of the neural hand representation may depend on recent Thumb use, additional analysis was conducted using a partial dataset acquired in a follow-up scan (7 to 10 days after the end of training) from a subgroup of available participants ($n = 12$). The original pre-post hand × time interaction remained significant even with this smaller subset of people [$F(1,417.99) = 4.8$, $P = 0.03$]. The initial difference between the pre- and post representation of the right (augmented) hand was ambiguous [$t(13.7) = 1.36$, $P = 0.19$, BF = 0.58]. We found moderate Bayesian evidence [$t(13.6) = 0.45$, $P = 0.66$, BF = 0.31] for a null difference between the distances measured during pre- and follow-up sessions, suggesting that in the follow-up scan, the reduction of the inter-finger distances was at least partially diminished. Note, however, that no significant difference between the augmented hand's representation in post- and follow-up scans was observed [$t(12.9) = 0.71$, $P = 0.5$, BF = 0.37].

Hand-toes functional relationship in the primary sensorimotor cortex remains stable

Last, we ran a series of analyses exploring the relationship between neural representations of the hands and the toes—the body part controlling the Thumb's movement. We first focused on primary sensorimotor cortex and found no significant changes relating to Thumb training (fig. S7). Specifically, we examined toes-specific net activity within the augmented hand's area [$t(19) = 0.47$, $P = 0.64$, BF = 0.26], dissimilarity between multivariate activity patterns elicited by hand and toes movements [hand × time interaction: $F(1,19) = 1.46$, $P = 0.24$, BF = 0.38] and functional coupling between sensorimotor hand and feet areas [resting state functional connectivity (*27*): $t(19) = 1.375$, $P = 0.185$, BF = 0.52]. These results suggest that although augmentation might promote plasticity locally (i.e., between fingers), the neural representation of the body at large remains unchanged in the primary sensorimotor cortex.

Finally, we examined inter–body part representations in the supplementary motor area (SMA), involved in motor learning and coordination (*28*). SMA contains a much cruder body map compared with the sensorimotor cortex (*28*), providing a better substrate for exploring changes to inter–body part relationships. Using cross-validated Mahalanobis distances, we found a significant reduction in the hand-toes distance after training, specific to the augmented (right) hand [$t(19) = 3.56$, $P = 0.002$, $\eta_p^2 = 0.4$] and resulting in a significant hand × time interaction [$F(1,19) = 9.13$, $P = 0.007$, $\eta_p^2 = 0.33$; Fig. 4]. We repeated this analysis with an additional body part unrelated to Thumb's control (lips) and again found a significant hand × time interaction [$F(1,19) = 9.1$, $P = 0.007$, $\eta_p^2 = 0.35$] with no significant three-way (hand × time × body part) interaction [$F(1,19) < 0.001$, $P = 0.99$, BF = 0.31]. In other words, the reduction in the inter–body part distance was similar across hand-toes and hand-lips. This finding suggests an overall decrease in selectivity that could be attributed to increased tonic inhibition, as examined in our computational simulation of the sensorimotor cortex (see Fig. 4).

DISCUSSION

Here, we provide a comprehensive demonstration of successful motor integration of a robotic augmentation device (the Third Thumb) and explore how augmentation influences the user's hand function and representation. After only 5 days of Thumb use, participants showed significant improvements in augmented hand motor performance across multiple tasks. In addition to individuated control of the extra Thumb, participants were able to integrate Thumb motor

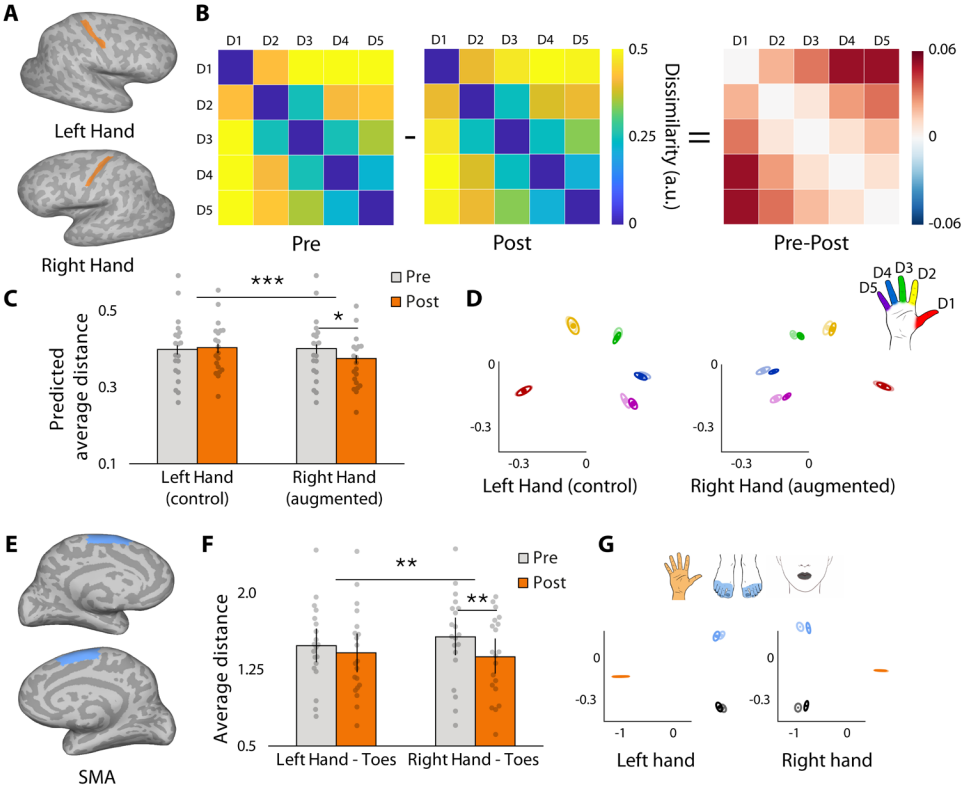

Fig. 3. Biological hand's representation shrinks after hand augmentation. (**A**) The sensorimotor hand area was defined anatomically, on the basis of a primary motor cortex segmentation. (**B**) Group mean dissimilarity matrix of the right (augmented) hand before and after training. Each cell shows the Mahalanobis (cross-validated) distance between the representational patterns of two fingers. a.u., arbitrary units. (**C**) The average inter-finger distances of the right (augmented) but not the left (nonaugmented) hand decreased significantly after Thumb use. The bars depict group mean, and error bars represent SEM. Individual dots correspond to individual participants' average distance as predicted by the LMM (see Materials and Methods). (**D**) MDS depiction of the left- and right-hand (augmented) representational structures. Ellipses indicate between-participant SEs. Darker colors represent the postscan, whereas lighter colors represent the pre (baseline) scan. Red, D1; yellow, D2; green, D3; blue, D4; purple, D5. (**E**) SMA ROI was defined anatomically, on the basis of segmentation of BA6. (**F**) The distance between the hand and the feet, quantified in SMA, decreases significantly for the right, but not the left hand. (**G**) MDS depiction of the inter–body part distances in the SMA. Darker colors represent the postscan, whereas lighter colors represent the pre (baseline) scan. Blue, toes; orange, hand; black, lips. Asterisks denote significant effects at $^{*}P < 0.05$, $^{**}P < 0.01$, and $^{***}P < 0.001$.

control with the movements of their natural hand, requiring collaboration, shared supervision, and hand-robot coordination. Motor performance was greatly improved even without visual feedback and remained stable under increased cognitive load, although note that increasing cognitive load demands even further is likely to eventually lead to increased interference with the motor performance (*21*). The ability to successfully coordinate between the Thumb and the biological hand across diverse task demands is crucial for successful adoption of augmentation devices. We further show that hand augmentation resulted in an increased explicit sense of embodiment over the Thumb, a key goal for successful augmentation (*29*), whereas implicit body image was found to be stable. By demonstrating successful adaptation to motor augmentation under diverse settings, our findings extend earlier pioneering proof-of-concept accounts of successful usage of extra robotic fingers (*1*, *4*, *6*, *30*–*32*) or arms (*3*, *5*) under restricted circumstances.

Successful adoption of augmentative technologies relies not only on the user's proficiency in operating the robotic device. A further challenge for augmentation is to ensure that the device usage will not influence the users' ability to control their biological body, especially when the augmentative device is not being used or even worn. Therefore, a critical question for safe motor augmentation is whether it would incur any changes to the user's biological body representation. This concern is rooted in previous research of brain plasticity, demonstrating that our motor experience shapes the structure and function of the nervous system (*10*, *33*). Hence, because motor augmentation is designed to change the way we interact with the environment, it is reasonable to predict that augmenting ourselves will reshape the neural basis of our biological body. Moreover, because we were not born with the innate capacity to control additional robotic body parts, successful motor augmentation likely requires extensive long-term practice, as highlighted in our training results. With that in mind, our investigation was focused on changes incurred to the body representation while the Thumb was not being operated. This approach allows for our findings to be generalized to other forms of robotic thumb control.

Traditionally, body representation in the sensorimotor cortex is considered to be highly adaptive even in the adult brain (*34*, *35*); however, recent research contributes a new perspective on its malleability (*13*, *14*). Tools have been suggested to update the biological body representation, for example, by tool-body integration (*36*–*38*). Yet, tools are normally used to replace the capacity of the hand, rather than to accompany it. Therefore, when using a tool, one is not required to radically alter their hand function (for example, the user will choose a grip for the tool's handle that fits the natural synergies of the fingers). Hence, tool use does not entail an updated representation of the hand itself. Conversely, motor augmentation invites the user to reinvent the way they use their own body. Consequently, here, motor integration of the Thumb altered the natural finger coordination patterns (kinematic synergies) of the augmented hand, with the augmentation group showing more complex movement patterns than the control group. This challenge is more closely akin to the acquisition of a new and complex motor skill, e.g., learning to play the piano. Recent research has demonstrated that long-term training leads to changes in finger representations (*39*). Specifically, trained pianists (over the course of many years, starting in childhood) demonstrate altered hand representation (lower inter-finger representational distances) relative to novices. This evidence further emphasizes the need to examine how long-term motor augmentation can influence biological hand representation.

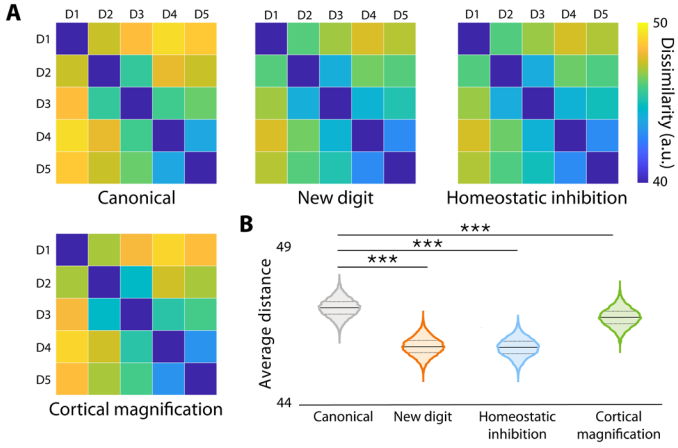

Fig. 4. Outcomes of the computational simulation. The adoption of an extra robotic thumb by an adult with a stable hand representation promotes a change to existing brain organization. Here, we used computational simulations to explore multiple potential plasticity mechanisms that could trigger the observed shrinkage of the hand representation. First, on the basis of information processing theories (*68*, *69*), the integration of a new additional finger into the hand's motor control could impinge on the existing representation of the biological fingers (new digit model). Second, the change in finger coordination, observed during training, may also lead to abrupt changes in excitability profiles that can trigger homeostatic plasticity mechanisms and promote increased tonic inhibition [homeostatic inhibition model (*70*)]. Third, the change to finger coordination may also result in increased finger individuation, leading to increased cortical representation of individual fingers via Hebbian learning [cortical magnification model (*71*)]. Simulating "neuronal activity" over a fixed-size ROI split into finger-specific areas, we found that each of these processes is conceptually capable of causing the observed reduction in representational selectivity. (**A**) Mean dissimilarity matrices computed from 10,000 simulations of each of the models. (**B**) Average distance (dissimilarity) is significantly decreased, as compared with the canonical hand representation in each of the models. Solid lines represent the mean of 10,000 simulations, and dotted lines denote the first and third quartile of the data. Asterisks denote significant effects at ***$P < 0.001$.

Here, we used a variety of pre- to post-measures to study changes in body representation when the Thumb was not being used, or even worn. Although some aspects of body representation (e.g., body image and large-scale connectivity profile) were found to be stable, semi-intensive Thumb usage (2.3 to 6.3 hours/day) resulted in mild yet significant changes to the hand representation. Specifically, we observed a shrinkage of the neural hand representation in the sensorimotor cortex. This is likely a consequence of the motor adaptations that the users made to best cooperate with the augmentation device (*10*, *40*, *41*), as further supported by the follow-up scan taken 7 to 10 days after Thumb usage had ceased. As mentioned in the introduction, inter-finger representation is highly stable even after intensive motor training, so long as this training does not introduce changed inter-finger coordination patterns (*16*). Conversely, shrinkage of inter-finger distances was recently reported in a finger "syndactyly" (a condition in which two or more fingers are fused together) study, causing abrupt and profound change to inter-finger coordination (*9*). The reduced inter-finger distance was associated with maladaptive perceptual consequences, i.e., reduced perceptual acuity to discriminate between tactile stimuli across the fingers. This is in stark contrast to a recent report of individuals who were born with a sixth (fully operational) finger and could harness processes of developmental plasticity to establish normal motor control across all six fingers (*42*).

As illustrated through the computational simulation shown in Fig. 4, our findings are compatible with both adaptive and maladaptive plasticity mechanisms. As we originally hypothesized, the shrinkage effect observed here could be disruptive, e.g., akin to other studies reporting neural correlates of decreased motor control (*18*). It could also result from homeostatic plasticity mechanisms aimed at stabilizing brain activity in the presence of abrupt input changes (*43*). This interpretation is supported by the reduced interbody part distances found in the SMA. Alternatively, the shrinkage effect could also be directed at establishing optimal representation of the Thumb relative to the rest of the augmented hand and, as such, involved in developing motor control over a new body part. For instance, by inducing new kinematic synergies, learning to use the extra Thumb may be pushing the network outside of its existing manifold (*44*) to allow for formation of new neural activity patterns. In other words, the observed neural changes could be reflective of a more compact, but not necessarily less functional, hand representation. At this early stage of research, it is not yet clear whether these changes are adaptive, maladaptive, or epiphenomenal. The behavioral evidence, examining the impact of hand augmentation on finger enslavement, was unfortunately too ambiguous to determine the answer to this key question (see fig. S5). Yet, regardless of the specific mechanism, our evidence nevertheless suggests that motor augmentation might incur some changes to the augmented hand's representation. Considering that neuroimaging results have previously been shown as reliable biomarkers for behavioral outcomes, relating to both motor control [e.g., in stroke recovery (*45*)] and pain (*46*), we believe that it is crucial to consider whether the observed neural shifts in the biological hand representation could be incurred safely (*29*).

To conclude, emerging technologies designed to assist, substitute, and even augment our motor abilities hold tremendous promise for transforming the lives of both disabled and healthy communities. Hand augmentation could benefit diverse groups of people, from factory workers to surgeons—allowing them to perform their labor more safely, without having to coordinate their movements with assistants or external devices—and from healthy individuals to those with temporary or chronic hand impairment (*1*), looking to improve decreased hand functionality. This vision depends not only on the exciting technological innovations but also critically relies on our brain's ability to learn, adapt, and interface with these devices. Therefore, as technology becomes more integrated with the human body, we see new challenges and opportunities emerging from neural and cognitive perspectives. Critical questions arise as to how such human-machine integration can be best achieved, given expected neurocognitive bottlenecks of brain plasticity. Here, we demonstrate that successful integration of motor augmentation can be readily achieved, with potential for flexible use, reduced cognitive reliance, and increased sense of embodiment. However, such successful human-robot integration may have direct consequences on key aspects of body representation and motor control, be it adaptive or maladaptive, which need to be understood and explored further before this technology can be widely implemented.

MATERIALS AND METHODS

Participants

Thirty-six healthy volunteers [23 females; mean age = 23.1 ± 3.89; all right handed; Edinburgh handedness inventory (EHI) score = 77.44 ± 23.98] were recruited from internet-based advertisements and randomly

assigned to either augmentation (n = 24; 14 females; mean age = 22.9 ± 4.12; EHI score = 80.52 ± 17.71) or control (n = 12; 9 females; mean age = 23.5 ± 3.55; EHI score = 71.83 ± 32.77) group. All participants were right handed, were between the ages of 18 and 35, did not have any known motor disorders, and reported no counterindications for MRI. Professional musicians were excluded from the study. Handedness was confirmed using the EHI. Ethical approval was granted by the University College London Research Ethics Committee (REC: 12921/001). All participants gave their written informed consent before participating in the study.

Because of scheduling conflicts, one control participant and three augmentation participants dropped out of the study. In addition, because of technical problems during data collection, one augmentation participant was discarded from the study.

Experimental design

To assess the effects of hand augmentation on body representation, we implemented a longitudinal experimental design (Fig. 1C), involving eight experimental sessions conducted across 7 to 9 days. All participants undertook (i) a 1-hour familiarization session, introducing the equipment and the behavioral tasks; (ii) a 4-hour baseline (pretest) session consisting of behavioral testing and an MRI scan; (iii) five 2-hour training sessions conducted over the five subsequent days (one session per day); and (iv) a final 4-hour posttest session corresponding to the baseline session. In addition, 12 of the participants from the augmentation group also undertook a secondary follow-up MRI session conducted 7 to 10 days after the end of training. Because the acquisition of the follow-up dataset was decided after the study onset, on the basis of the preliminary results, we were unable to collect the data from all of the study participants. Because of scheduling issues, one augmentation participant and one control participant completed only four of five training sessions.

All study participants were asked to wear an extra robotic thumb (the Third Thumb; Fig. 1, A and B) on their right hand throughout the day. Participants were instructed to wear the Thumb during the in-lab training sessions and to continue wearing it outside of the lab for at least 4 hours per day. The augmentation group had full motor control over the Thumb and needed to actively use it to complete the training tasks. They were also encouraged to use it as much as possible outside of the lab for a freestyle environment exploration ("in the wild"). The control group wore a static (not moving) version of the Thumb and completed the training tasks without being able to control it. Because of initial equipment issues, the first two control participants did not wear the Thumb during training.

Usage measures in the wild

To monitor Thumb usage outside the lab, self-reported wear time and Thumb usage examples were collected daily from all wearers/users. Daily reports were averaged across days, and an independent samples t test was used to test for differences in wear time between the augmentation and control group. In addition, both pressure sensors were equipped with an SD card data logger. While the Thumb was on, both sensors were logging the corresponding motor's position and the associated time stamp to the SD cards. If the participant turned the Thumb off during the day, then the recording was paused and resumed after the motor was restarted. Those recordings were used to further quantify the number of hours that participants spent using the Thumb per day. Use time was defined as the time spent wearing the extra Thumb with the motors of the Thumb switched on, whereas movement time was defined as the time spent actively exerting pressure with the big toes while the Thumb was switched on. Because of initial equipment issues, the sensors' data from first three augmentation participants were not recorded.

Training protocol

During the training sessions, participants were asked to complete a set of reaching and grasping tasks. These tasks were designed to encourage the use of the Thumb and allow the participants to develop complex hand-robot interactions. The task execution was restricted to the augmented (right) hand. The augmentation group was instructed to use the extra Thumb to complete the training tasks. The control group, wearing the static version of the Thumb, was instructed to complete the training tasks using only their natural fingers, i.e., without using the Thumb. Training tasks required participants to (i) use the Thumb in collaboration with another finger to pick up multiple objects (collaboration, e.g., building a tower), (ii) use the Thumb to extend the natural grip of the hand and to free up the use of the biological fingers (shared supervision, e.g., stirring cups), (iii) use the Thumb individually while having their hand occupied with task-irrelevant objects (individuation, e.g., stacking tapes), or (iv) oppose the robotic Thumb to one of the natural fingers (hand-Thumb coordination). For all of the tasks, participants were seated at a desk facing the camera, recording their hand movements. Each task was conducted for 10 to 15 min and repeated on two to four separate training days, with the exception of the hand robot coordination task (see the Supplementary Materials), which was performed during each of the training sessions.

To quantify the improvement of the augmentation group on each of the training tasks, the outcome measure of each task was averaged for each participant and each training session. Because different participants had slightly different training regimes, in terms of distribution of tasks across the days, we sorted the average scores on the basis of the order of task repetition (i.e., first, second, and third time the task was repeated regardless of which days it was repeated on). These data were then analyzed using a repeated-measures analysis of variance (ANOVA) in SPSS.

Numerical cognition

To assess the cognitive load related to Thumb use, a numerical cognition task was performed twice, in the first and the last training session (*21*). The task was adapted from previous studies showing that numerical cognition influences motor performance while controlling a virtual prosthetic arm (*22*) or a brain-computer interface (*47*). Participants were asked to perform a collaboration task, building a tower (see the Supplementary Materials), while simultaneously presented with a set of low- and high-pitch auditory tones played from a laptop. The tones were presented every 1 to 6 s in a randomized order, for a total duration of 1 min per block. Starting with a number 10, participants were instructed to add 1 to the current number after hearing a high tone and subtract 1 from the current number after hearing a low tone. After each mathematical operation, participants were instructed to verbally respond with the resulting number. To assure participants' engagement with the dual task, participants were explicitly instructed to pay closer attention to the arithmetic operations, treating the motor task (building a tower) as a secondary task. Participants performed five blocks of the numerical cognition task during each session. Numerical cognition blocks were always preceded and followed by five blocks of normal

(baseline) building a tower task (five baseline blocks, five numerical cognition blocks, and five baseline blocks). Note that the first three participants did not complete the numerical cognition task.

For each participant, the average number of tower floors built was calculated from all the numerical cognition blocks in which the correct mathematical operations were performed. Trials in which a wrong number was given were discarded (on average, 15 to 19% of the trials were discarded per participant). Note, however, that similar results were obtained when including the erroneous trials (see fig. S3). To determine whether the extra cognitive load caused by the numerical cognition task had any impact on participants' motor performance when using the extra Thumb, the average score from the numerical cognition task was compared with the baseline score. This was done separately for the first and the last day of training. The baseline score was calculated as the average number of tower floors built across the two baseline blocks (10 trials) that proceeded and followed the numerical cognition task.

Tracking hand movements

To assess the changes in finger coordination across all training tasks, we tracked the kinematics of the augmented (right) hand using flex sensors embedded in a dataglove (CyberGlove, Virtual Technologies, Palo Alto, CA, USA). Note that finger kinematics have been previously shown to reflect the brain organization better than electromyography-derived measures (*10*). Here, the sensors of the dataglove were associated with 19 degrees of freedom and measured the joint angles of the metacarpal-phalangeal (MCP), proximal interphalangeal (PIP), and distal interphalangeal joints of the four fingers; the carpometacarpal, MCP, and interphalangeal joint of the biological thumb; the three relative abduction angles between the four fingers; and the abduction angle between the biological thumb and the palm of the hand. Sensors were sampled continuously at 100 Hz using Shadow Robot's (www.shadowrobot.com) CyberGlove interface for the Robot Operating System (ROS; www.ros.org).

Participants wore the CyberGlove underneath the extra Thumb throughout all of the training sessions. Kinematics associated with each of the training tasks performed during a given session were recorded onto a separate file. CyberGlove was calibrated for each participant at the beginning of each training session, using a min-max pose calibration procedure provided with the ROS CyberGlove package (see the Supplementary Materials). Because of initial equipment issues, the first four augmentation participants did not wear the CyberGlove during training.

Hand kinematics analysis

We focused the hand kinematics analysis on the data recorded during the first and last days of training. The joint angles were smoothed using a third-order Savitzky-Golay filter, with a window length of 151 samples. Angular velocities were then calculated from the first difference of the filtered joint angle data divided by the time step. Because most of the finger movements used during the training tasks were executed using the PIP joints, to simplify the analysis (*10*), only the data from these five joints were analyzed, resulting in five time series signals per session per participant. Because of acquisition errors, for two augmentation participants and two control participants, the data recorded during the first day of training were unavailable. Therefore, for these participants, the data from the second day of training were used instead. Similarly, when the data from the last day of training were unavailable (three augmentation participants and two control participants), the data from the penultimate day of training were used instead. Because of calibration issues, the hand kinematics data of one augmentation and two control participants were discarded from all the subsequent analysis.

To quantify the complexity of the hand movements across both groups, we first conducted a PCA of the angular velocities of the PIP joints. For each participant and session, the five angular velocities were z-normalized (*48*) and decomposed into participant- and session-specific kinematic synergies using PCA. Five PCs were computed for each participant and session. The extracted PCs were matched across participants using normalized scalar product (dot product) and ordered according to the amount of variance explained by each component. Consistent with the literature (*49*, *50*), we found that the first PC accounted for more than 40% of total variance and reflected a coordinated movement of all the fingers (see fig. S4 for all the PCs). To quantify the dimensionality of the hand movements, for each participant and day, we recorded the number of PCs needed to explain 80% of total variance (*51*). These were then compared across groups in a repeated-measures ANOVA with time (days 1 and 5) as a within-participants factor and group (augmentation and control) as between-participants factor. To quantify the contribution of the all-digit movements to the complexity of the hand kinematics, we compared the amount of variance explained by the first PC across both groups using the same repeated-measures ANOVA design.

Next, to interrogate more detailed changes to the finger cooperation pattern caused by the hand augmentation, we looked at the degree of coupling between digit pairs, adapting the methods used in (*49*). We used linear regression to fit the angular velocity data of a given digit as a function of the angular velocity of each of the other digits individually. This yielded a single determination coefficient (R^2) for each digit pair, expressing the proportion of total variance of each digit's angular velocity that could be explained by a linear reconstruction, based on its paired regression with each of the other digits. A qualitative comparison between the results obtained from the control group (who did not use the Thumb during the training) and the outcomes of previous hand kinematics research conducted during free movement (*10*, *49*) confirmed that the conducted analysis resulted in a typical finger synergy profile.

To assess the effect of Thumb use on the finger coordination profile across groups, we performed a linear mixed model (LMM) analysis with fixed factors of time, group (augmentation versus controls), and digit pair; a random effect of participant; and a random participant-specific slope of time. The LMM was evaluated in R (version 3.5.2) under restricted maximum likelihood (REML) conditions with Satterthwaite adjustment for the degrees of freedom.

Pre-post testing protocol

To assess the neural correlates of hand augmentation, we used a set of pre- to post comparison measures, consisting of both behavioral and neuroimaging tasks. To characterize the emerging representation of the extra Thumb, we probed the proprioception and motor control of the Thumb using a sequential variation of the hand-Thumb coordination task. We also assessed the perceived (explicit) embodiment of the Thumb using questionnaires. To interrogate changes to the natural hand representation, we measured biological finger codependencies using finger kinematics and force enslavement (see the Supplementary Materials). Changes to body image were probed using tactile distance and hand laterality

judgment tasks (see the Supplementary Materials). Last, fMRI was used to track the hand representation in the sensorimotor cortex of the brain and to interrogate changes to the relationship between the hand and feet representations. With the exception of the hand-Thumb coordination task, participants were not wearing the Thumb during testing.

Hand-Thumb coordination (sequential)

To probe changes to implicit motor control of the Thumb, a sequential variation of the hand-Thumb coordination (finger-to-Thumb opposition) task has been used. In this task, participants sequentially opposed the Thumb to the tip of each of the five fingers of their augmented hand, starting with the little finger. Participants were instructed to repeat this movement cycle as many times as possible within a 1-min block, while maintaining high accuracy. The task consisted of five blocks. To assess the proprioception of the Thumb, participants were further asked to perform five blocks of the same task while blindfolded. The experimenter recorded the number of successful hits per block. For each participant, an average score (number of hits) was calculated separately for each session (pre and post) and vision condition (with vision and blindfolded). Because of a data acquisition mistake, one control participant was not included in the analysis.

Embodiment questionnaires

To assess changes in the embodiment of the Thumb, participants were asked to complete an embodiment questionnaire before the first and again after the last training session (Table 1). The questionnaire was focused on the explicit (phenomenological) aspect of embodiment, concerned with whether the extra Thumb feels like a part of one's hand (*52*). Because of data collection issues, five augmentation participants and one control participant only completed the post-training embodiment questionnaire. Participants were asked to rate their agreement with 12 statements [based on (*24*)] on a seven-point Likert-type scale ranging from −3 (strongly disagree) to +3 (strongly agree). Statements were clustered into four main categories, probing different aspects of embodiment, namely, body ownership, agency, body image, and somatosensation.

For each participant, questionnaire scores were averaged within each embodiment category. Note that in the body ownership category, the opposite (negative) value of the "foreign body" statement has been used while computing the average. One augmentation participant was discarded from this analysis because their averaged agency score was classified as a statistical outlier (different from the mean score by more than 3 SDs).

Statistical analysis

All statistical analysis was performed using IBM SPSS Statistics for Macintosh (version 24), R (for LMMs), and JASP (version 0.11.1). Tests for normality were carried out using a Shapiro-Wilk test. Training data that were not normally distributed were log-transformed before further statistical analysis. With the exception of hand kinematics and force enslavement datasets, which were analyzed using LMMs, all the within-group comparisons were carried out using paired *t* tests or repeated-measures ANOVAs (training task data). Between-group comparisons were carried out using ANCOVAs with group (augmentation and controls) as a fixed effect and the prescore used as a covariate (*53*). All nonsignificant results were further examined using corresponding Bayesian tests under continuous prior distribution (Cauchy prior width $r = 0.707$).

Table 1. Embodiment questions divided into four separate embodiment categories.

Body ownership
1."It seems like the robotic finger belongs to me."
2."It seems like the robotic finger is a part of my hand."
3."It seems like the robotic finger is a part of my body."
4."It seems like the robotic finger is a foreign body." (negative)
5."It seems like the robotic finger is fused with my body."
6."It seems like I have six fingers."
Agency
1."It seems like I can move the robotic finger if I want."
2."It seems like I am in control of the robotic finger."
Body image
1."It seems like I am looking directly at my own finger, rather than a prosthesis."
2."It seems like the robotic finger begins to resemble my other fingers."
Somatosensation
1."I can feel temperature in the robotic finger."
2."I can feel the posture of the robotic finger."

Scanning procedures

Both pre- and post-neuroimaging sessions were composed of the following functional scans: (i) a resting state scan (see the Supplementary Materials), (ii) a motor localizer scan (see the Supplementary Materials), and (iii) four finger-mapping scans. In addition, a structural scan and field maps were obtained during each scanning session.

Finger-mapping scans

Participants were instructed to perform visually cued movements of individual digits of either hand, bilateral toe movements, and lips movements. The different movement conditions, as well as rest periods, were presented in 9-s blocks. The individual digit movements were performed in the form of button presses on MRI-compatible button boxes (four buttons per box) secured on the participant's thighs. The movements of either of the (biological) thumbs were performed by tapping them against the wall of the button box. Instructions were delivered via a visual display projected into the scanner bore. Ten vertical bars, representing the fingers, flashed individually in green at a frequency of 1 Hz, instructing movements of a specific digit at that rate. Toe and lips movements were cued by flashing the words "Feet" or "Lips" at the same rate of 1 Hz. Each condition was repeated four times within each run in a semicounterbalanced order. Participants performed four runs of this task. Because of timing issues, three augmentation participants and one control participant completed only three runs of the finger-mapping task. In addition, because of a data acquisition issue, the finger-mapping data of one control participant were discarded.

MRI data acquisition

MRI images were acquired using a 3T Prisma MRI scanner (Siemens, Erlangen, Germany) with a 32-channel head coil. Functional images were collected using a multiband T2*-weighted pulse sequence with

a between-slice acceleration factor of 4 and no in-slice acceleration. This provided the opportunity to acquire data with high spatial (2 mm isotropic) and temporal (TR, 1450 ms) resolution, covering the entire brain. The following acquisition parameters were used: echo time (TE), 35 ms; flip angle, 70°; 72 transversal slices. Field maps were acquired for field unwarping. A T1-weighted sequence (Magnetization Prepared Rapid Gradient Echo, MPRAGE) was used to acquire an anatomical image (TR, 2530 ms; TE, 3.34 ms; flip angle, 7°; spatial resolution, 1 mm isotropic).

MRI analysis

MRI analysis was implemented using tools from Oxford Centre for Functional Magnetic Resonance Imaging of the Brain (FMRIB) Software Library [FSL (*54*, *55*)] and Connectome Workbench (humanconnectome.org) software, in combination with MATLAB scripts (version R2016a), both developed in-house [including FSL-compatible representational similarity analysis (RSA) toolbox (*56*)] and as part of the RSA Toolbox (*26*). Cortical surface reconstructions were produced using FreeSurfer [(*57*, *58*); freesurfer.net].

fMRI preprocessing

Functional data was first pre-preprocessed using FSL-FEAT (version 6.00). Preprocessing included motion correction using Motion Correction using FMRIB's Linear Image Registration Tool [MCFLIRT (*59*)], brain extraction using Brain Extraction Tool [BET (*60*)], temporal high-pass filtering, with a cutoff of 150 s for the finger-mapping scans and 100 s for resting-state and motor localizer scans, and spatial smoothing using a Gaussian kernel with a full width at half maximum of 3 mm for the finger-mapping scans and 5 mm for resting-state and motor localizer scans.

To make sure that the scans from the two scanning sessions were well aligned, for each participant, we calculated a midspace between their pre- and postscans, i.e., the average space in which the images are minimally reoriented. Each scan was then aligned to this pre-post midspace using FLIRT (*59*, *61*). See the Supplementary Materials for details.

Low-level task-based analysis

For task-based datasets, voxel-wise general linear model (GLM) analysis was carried out using FMRI Expert Analysis Tool (FEAT) to identify activity patterns related to the movement of each digit/body part. The design was convolved with a double-gamma hemodynamic response function and its temporal derivative. The six-motion parameters were included as regressors of no interest. In case of large movement between volumes (>1 mm), additional regressors of no interest were included in the GLM to account for each of these instances individually.

For the finger-mapping scans, 14 contrasts were set up: each digit versus rest, all left/right hand digits against rest, feet against rest, and lips against rest. The estimates from the four finger-mapping scans were then averaged voxel wise using fixed effects model with a cluster forming z threshold of 3.1 and family-wise error corrected cluster significance threshold of $P < 0.05$, creating 14 main activity patterns for each session and participant.

For the motor localizer scans, four main contrasts were set up: right/left hand against lips and right/left foot against lips. The activity patterns associated with those four contrasts were then used to define functional regions of interest (functional ROIs; see the Supplementary Materials).

ROI definition

Changes to representational structure of the hand were studied using anatomical ROIs, as previously practiced in related studies (*14*, *62*, *63*). Structural T1 images, registered to the structural midspace, were used to reconstruct the pial and white-gray matter surfaces using FreeSurfer. Surface co-registration across hemispheres and participants was done using spherical alignment. Individual surfaces were nonlinearly fitted to a template surface, first in terms of the sulcal depth map and then in terms of the local curvature, resulting in an overlap of the fundus of the central sulcus across participants (*64*). The anatomical sensorimotor ROI, used for the multivariate analysis, was defined on the group surface using probabilistic cytotectonic maps aligned to the average surface (*65*). This ROI was then projected into the individual brains via the reconstructed individual anatomical surfaces. Because we were primarily interested in the motor representation of the hand, we focused our anatomical ROI on M1, selecting all surface nodes with the highest probability for Brodmann area 4 (BA4) spanning a 2-cm strip medial/lateral to the anatomical hand knob (*14*, *66*). However, we note that, given the probabilistic nature of these masks, the dissociation between S1 and M1 is only an estimate, and thus, our ROI should be treated as a sensorimotor one. SMA was defined as all surface nodes along the medial wall with the highest probability for BA6 (*16*, *17*).

For our univariate analyses (resting state connectivity and net activity analysis), we also defined a separate set of functional ROIs based on the sensorimotor representations of the left/right hand and feet of each participant. See the Supplementary Materials for details.

Multivariate representational structure of the hand (RSA)

We used RSA (*67*) to assess the multivariate relationships between the activity patterns generated across digits and sessions. RSA was also used to quantify dissimilarity between multivariate activity patterns elicited by hand and toe movements (see the Supplementary Materials). The dissimilarity between activity patterns within the M1 anatomical hand ROI was measured for each digit pair using the cross-validated squared Mahalanobis distance (*26*). We calculated the distances using each possible pair of imaging runs within a single scanning session (pre and post) and then averaged the resulting distances across run pairs. Before estimating the dissimilarity for each pattern pair, the activity patterns were prewhitened using the residuals from the GLM. Because of the cross-validation procedure, the expected value of the distance is zero (or below) if two patterns are not statistically different from each other and larger than zero if the two representational patterns are different. The resulting 10 unique interdigit representational distances were put together in a representational dissimilarity matrix (RDM).

To assess the effect of 5-day Thumb usage on the overall representation structure (dissimilarity), we performed an LMM analysis with fixed factors of time, hand, and digit pair; a random effect of participant; and a random participant-specific slope of time. The LMM was evaluated in R (version 3.5.2) under REML conditions with Satterthwaite adjustment for the degrees of freedom.

As an aid to visualizing the RDMs, we also used classical multidimensional scaling (MDS). MDS projects the higher-dimensional RDM into a lower-dimensional space, while preserving the interdigit dissimilarity values as well as possible. MDS was performed on data from individual participants and averaged after Procrustes

alignment (without scaling) to remove arbitrary rotation induced by MDS. Note that MDS is presented for intuitive visualization purposes only and was not used for statistical analysis.

SUPPLEMENTARY MATERIALS

robotics.sciencemag.org/cgi/content/full/6/54/eabd7935/DC1
Materials and Methods
Table S1. Parameters used for the numerical simulation of cortical magnification, homeostatic inhibition, and addition of a new digit.
Fig. S1. Force sensors setup.
Fig. S2. Training outcomes in augmentation (orange) and control (blue) groups.
Fig. S3. Motor performance with the Thumb is not influenced by the additional cognitive load (numerical cognition task).
Fig. S4. Kinematic synergies captured during Thumb use.
Fig. S5. Outcomes of the force enslavement testing.
Fig. S6. Biological hand's representation of the control groups remains stable.
Fig. S7. Hand-toes functional relationship in the primary sensorimotor cortex remains stable.
Movie S1. Examples of the in-lab training tasks.
References (*72*–*82*)

REFERENCES AND NOTES

1. G. Salvietti, I. Hussain, D. Cioncoloni, S. Taddei, S. Rossi, D. Prattichizzo, Compensating hand function in chronic stroke patients through the robotic sixth finger. *IEEE Trans. Neural Syst. Rehabil. Eng.* **25**, 142–150 (2017).
2. F. Y. Wu, H. H. Asada, Supernumerary robotic fingers: An alternative upper limb prosthesis, in *Proceedings of the ASME Dynamic Systems and Control Conference (DSCC)*, San Antonio, TX, October 2014.
3. T. Sasaki, M. H. D. Y. Saraiji, C. L. Fernando, K. Minamizawa, M. Inami, MetaLimbs: Multiple arms interaction metamorphism, paper presented at the ACM SIGGRAPH 2017 Emerging Technologies, Los Angeles, CA, 30 July to 3 August 2017.
4. N. S. Meraz, M. Sobajima, T. Aoyama, Y. Hasegawa, Modification of body schema by use of extra robotic thumb. *Robomech J.* **5**, 3 (2018).
5. C. I. Penaloza, S. Nishio, BMI control of a third arm for multitasking. *Sci. Robot.* **3**, eaat1228 (2018).
6. A. Shafti, S. Haar, R. M. Zaldivar, P. Guilleminot, A. A. Faisal, Learning to play the piano with the Supernumerary Robotic 3rd Thumb. *bioRxiv*, 2020.05.21.108407 (2020).
7. M. J. Arcaro, P. F. Schade, M. S. Livingstone, Body map proto-organization in newborn macaques. *Proc. Natl. Acad. Sci. U.S.A.* **116**, 24861–24871 (2019).
8. S. Dall'Orso, J. Steinweg, A. G. Allievi, A. D. Edwards, E. Burdet, T. Arichi, Somatotopic mapping of the developing sensorimotor cortex in the preterm human brain. *Cereb. Cortex* **28**, 2507–2515 (2018).
9. J. Kolasinski, T. R. Makin, Perceptually relevant remapping of human somatotopy in 24 hours. *eLife* **5**, e17280 (2016).
10. N. Ejaz, M. Hamada, J. Diedrichsen, Hand use predicts the structure of representations in sensorimotor cortex. *Nat. Neurosci.* **18**, 1034–1040 (2015).
11. S. N. Flesher, J. L. Collinger, S. T. Foldes, J. M. Weiss, J. E. Downey, E. C. Tyler-Kabara, S. J. Bensmaia, A. B. Schwartz, M. L. Boninger, R. A. Gaunt, Intracortical microstimulation of human somatosensory cortex. *Sci. Transl. Med.* **8**, 361ra141 (2016).
12. F. Mancini, A. P. Wang, M. M. Schira, Z. J. Isherwood, J. H. McAuley, G. D. Iannetti, M. I. Sereno, G. L. Moseley, C. D. Rae, Fine-grained mapping of cortical somatotopies in chronic complex regional pain syndrome. *J. Neurosci.* **39**, 9185–9196 (2019).
13. S. Kikkert, J. Kolasinski, S. Jbabdi, I. Tracey, C. F. Beckmann, H. Johansen-Berg, T. R. Makin, Revealing the neural fingerprints of a missing hand. *eLife* **5**, e15292 (2016).
14. D. B. Wesselink, F. M. van den Heiligenberg, N. Ejaz, H. Dempsey-Jones, L. Cardinali, A. Tarall-Jozwiak, J. Diedrichsen, T. R. Makin, Obtaining and maintaining cortical hand representation as evidenced from acquired and congenital handlessness. *eLife* **8**, e15292 (2019).
15. M. Bruurmijn, I. P. L. Pereboom, M. J. Vansteensel, M. A. H. Raemaekers, N. F. Ramsey, Preservation of hand movement representation in the sensorimotor areas of amputees. *Brain* **140**, 3166–3178 (2017).
16. P. Beukema, J. Diedrichsen, T. D. Verstynen, Binding during sequence learning does not alter cortical representations of individual actions. *J. Neurosci.* **39**, 6968–6977 (2019).
17. E. Berlot, N. J. Popp, J. Diedrichsen, A critical re-evaluation of fMRI signatures of motor sequence learning. *eLife* **9**, e55241 (2020).
18. T. Elbert, V. Candia, E. Altenmuller, H. Rau, A. Sterr, B. Rockstroh, C. Pantev, E. Taub, Alteration of digital representations in somatosensory cortex in focal hand dystonia. *Neuroreport* **9**, 3571–3575 (1998).
19. N. Ejaz, A. Sadnicka, T. Wiestler, K. Butler, M. Edwards, J. Diedrichsen, Finger representations in sensorimotor cortex are not disrupted in musicians' dystonia, paper presented at the Society for Neuroscience Annual Meeting, San Diego, CA, 12 to 16 November 2016.
20. D. Clode, The Third Thumb (2018); www.daniclodedesign.com/thethirdthumb.
21. H. J. Huang, V. S. Mercer, Dual-task methodology: Applications in studies of cognitive and motor performance in adults and children. *Pediatr. Phys. Ther.* **13**, 133–140 (2001).
22. H. J. Witteveen, L. de Rond, J. S. Rietman, P. H. Veltink, Hand-opening feedback for myoelectric forearm prostheses: Performance in virtual grasping tasks influenced by different levels of distraction. *J. Rehabil. Res. Dev.* **49**, 1517–1526 (2012).
23. R. O. Maimon-Mor, E. Obasi, J. Lu, N. Odeh, S. Kirker, M. MacSweeney, S. Goldin-Meadow, T. R. Makin, Communicative hand gestures as an implicit measure of artificial limb embodiment and daily usage. *medRxiv* 2020.03.11.20033928 (2020).
24. M. R. Longo, F. Schuur, M. P. Kammers, M. Tsakiris, P. Haggard, What is embodiment? A psychometric approach. *Cognition* **107**, 978–998 (2008).
25. F. de Vignemont, Body schema and body image—Pros and cons. *Neuropsychologia* **48**, 669–680 (2010).
26. H. Nili, C. Wingfield, A. Walther, L. Su, W. Marslen-Wilson, N. Kriegeskorte, A toolbox for representational similarity analysis. *PLoS Comput. Biol.* **10**, e1003553 (2014).
27. P. Kieliba, S. Madugula, N. Filippini, E. P. Duff, T. R. Makin, Large-scale intrinsic connectivity is consistent across varying task demands. *PLOS ONE* **14**, e0213861 (2019).
28. J. Ruan, S. Bludau, N. Palomero-Gallagher, S. Caspers, H. Mohlberg, S. B. Eickhoff, R. J. Seitz, K. Amunts, Cytoarchitecture, probability maps, and functions of the human supplementary and pre-supplementary motor areas. *Brain Struct. Funct.* **223**, 4169–4186 (2018).
29. T. R. Makin, F. de Vignemont, A. A. Faisal, Neurocognitive barriers to the embodiment of technology. *Nat. Biomed. Eng.* **1**, 0014 (2017).
30. F.Y. Wu, H.H. Asada, Bio-artificial synergies for grasp posture control of supernumerary robotic fingers, in *Proceedings of Robotics: Science and Systems X* (Berkeley, CA, 2014).
31. J. Cunningham, A. Hapsari, P. Guilleminot, A. Shafti, A. A. Faisal, The supernumerary robotic 3rd thumb for skilled music tasks, in *2018 7th IEEE International Conference on Biomedical Robotics and Biomechatronics (Biorob)* (IEEE, 2018), pp. 665–670.
32. Y. Zhu, T. Ito, T. Aoyama, Y. Hasegawa, Development of sense of self-location based on somatosensory feedback from finger tips for extra robotic thumb control. *ROBOMECH J.* **6**, 7 (2019).
33. H. Dempsey-Jones, D. B. Wesselink, J. Friedman, T. R. Makin, Organized toe maps in extreme foot users. *Cell Rep.* **28**, 2748–2756.e4 (2019).
34. M. M. Merzenich, J. H. Kaas, J. Wall, R. J. Nelson, M. Sur, D. Felleman, Topographic reorganization of somatosensory cortical areas 3b and 1 in adult monkeys following restricted deafferentation. *Neuroscience* **8**, 33–55 (1983).
35. R. J. Nudo, G. W. Milliken, W. M. Jenkins, M. M. Merzenich, Use-dependent alterations of movement representations in primary motor cortex of adult squirrel monkeys. *J. Neurosci.* **16**, 785–807 (1996).
36. A. Iriki, M. Tanaka, Y. Iwamura, Coding of modified body schema during tool use by macaque postcentral neurones. *Neuroreport* **7**, 2325–2330 (1996).
37. A. Maravita, A. Iriki, Tools for the body (schema). *Trends Cogn. Sci.* **8**, 79–86 (2004).
38. L. E. Miller, L. Montroni, E. Koun, R. Salemme, V. Hayward, A. Farne, Sensing with tools extends somatosensory processing beyond the body. *Nature* **561**, 239–242 (2018).
39. K. Ogawa, K. Mitsui, F. Imai, S. Nishida, Long-term training-dependent representation of individual finger movements in the primary motor cortex. *Neuroimage* **202**, 116051 (2019).
40. M. S. Graziano, T. N. Aflalo, Mapping behavioral repertoire onto the cortex. *Neuron* **56**, 239–251 (2007).
41. H. Dempsey-Jones, V. Harrar, J. Oliver, H. Johansen-Berg, C. Spence, T. R. Makin, Transfer of tactile perceptual learning to untrained neighboring fingers reflects natural use relationships. *J. Neurophysiol.* **115**, 1088–1097 (2016).
42. C. Mehring, M. Akselrod, L. Bashford, M. Mace, H. Choi, M. Bluher, A. S. Buschhoff, T. Pistohl, R. Salomon, A. Cheah, O. Blanke, A. Serino, E. Burdet, Augmented manipulation ability in humans with six-fingered hands. *Nat. Commun.* **10**, 2401 (2019).
43. D. Muret, T. R. Makin, The homeostatic homunculus: Rethinking deprivation-triggered reorganisation. *Curr. Opin. Neurobiol.* **67**, 115–122 (2020).
44. E. R. Oby, M. D. Golub, J. A. Hennig, A. D. Degenhart, E. C. Tyler-Kabara, B. M. Yu, S. M. Chase, A. P. Batista, New neural activity patterns emerge with long-term learning. *Proc. Natl. Acad. Sci. U.S.A.* **116**, 15210–15215 (2019).
45. C. M. Stinear, Prediction of motor recovery after stroke: Advances in biomarkers. *Lancet Neurol.* **16**, 826–836 (2017).
46. K. H. Brodersen, K. Wiech, E. I. Lomakina, C. S. Lin, J. M. Buhmann, U. Bingel, M. Ploner, K. E. Stephan, I. Tracey, Decoding the perception of pain from fMRI using multivariate pattern analysis. *Neuroimage* **63**, 1162–1170 (2012).
47. M. D. Guthrie, L. J. Brane, A. J. Herrera, M. L. Boninger, J. L. Collinger, The effect of distraction on intracortical brain-computer interface (BCI) performance, paper presented at the American Association of Physical Medicine and Rehabilitation Annual Meeting, San Antonio, TX, 14 to 17 November 2019.
48. N. J. Jarque-Bou, A. Scano, M. Atzori, H. Muller, Kinematic synergies of hand grasps: A comprehensive study on a large publicly available dataset. *J. Neuroeng. Rehabil.* **16**, 63 (2019).

49. J. N. Ingram, K. P. Kording, I. S. Howard, D. M. Wolpert, The statistics of natural hand movements. *Exp. Brain Res.* **188**, 223–236 (2008).
50. M. Santello, M. Flanders, J. F. Soechting, Postural hand synergies for tool use. *J. Neurosci.* **18**, 10105–10115 (1998).
51. N. Lambert-Shirzad, H. F. Van der Loos, On identifying kinematic and muscle synergies: A comparison of matrix factorization methods using experimental data from the healthy population. *J. Neurophysiol.* **117**, 290–302 (2017).
52. F. de Vignemont, Embodiment, ownership and disownership. *Conscious. Cogn.* **20**, 82–93 (2011).
53. G. J. P. Van Breukelen, ANCOVA versus change from baseline: More power in randomized studies, more bias in nonrandomized studies [corrected]. *J. Clin. Epidemiol.* **59**, 920–925 (2006).
54. M. Jenkinson, C. F. Beckmann, T. E. Behrens, M. W. Woolrich, S. M. Smith, FSL. *Neuroimage* **62**, 782–790 (2012).
55. S. M. Smith, M. Jenkinson, M. W. Woolrich, C. F. Beckmann, T. E. Behrens, H. Johansen-Berg, P. R. Bannister, M. De Luca, I. Drobnjak, D. E. Flitney, R. K. Niazy, J. Saunders, J. Vickers, Y. Zhang, N. De Stefano, J. M. Brady, P. M. Matthews, Advances in functional and structural MR image analysis and implementation as FSL. *Neuroimage* **23** (Suppl. 1), S208–S219 (2004).
56. D. Wesselink, R. Maimon-Mor, rsatoolbox, version 20fbe05 (2017); https://github.com/ronimaimon/rsatoolbox.
57. B. Fischl, A. Liu, A. M. Dale, Automated manifold surgery: Constructing geometrically accurate and topologically correct models of the human cerebral cortex. *IEEE Trans. Med. Imaging* **20**, 70–80 (2001).
58. A. M. Dale, B. Fischl, M. I. Sereno, Cortical surface-based analysis. I. Segmentation and surface reconstruction. *Neuroimage* **9**, 179–194 (1999).
59. M. Jenkinson, P. Bannister, M. Brady, S. Smith, Improved optimization for the robust and accurate linear registration and motion correction of brain images. *Neuroimage* **17**, 825–841 (2002).
60. S. M. Smith, Fast robust automated brain extraction. *Hum. Brain Mapp.* **17**, 143–155 (2002).
61. M. Jenkinson, S. Smith, A global optimisation method for robust affine registration of brain images. *Med. Image Anal.* **5**, 143–156 (2001).
62. S. A. Arbuckle, A. Yokoi, J. A. Pruszynski, J. Diedrichsen, Stability of representational geometry across a wide range of fMRI activity levels. *Neuroimage* **186**, 155–163 (2019).
63. A. Yokoi, S. A. Arbuckle, J. Diedrichsen, The role of human primary motor cortex in the production of skilled finger sequences. *J. Neurosci.* **38**, 1430–1442 (2018).
64. B. Fischl, N. Rajendran, E. Busa, J. Augustinack, O. Hinds, B. T. Yeo, H. Mohlberg, K. Amunts, K. Zilles, Cortical folding patterns and predicting cytoarchitecture. *Cereb. Cortex* **18**, 1973–1980 (2008).
65. T. Wiestler, J. Diedrichsen, Skill learning strengthens cortical representations of motor sequences. *eLife* **2**, e00801 (2013).
66. T. A. Yousry, U. D. Schmid, H. Alkadhi, D. Schmidt, A. Peraud, A. Buettner, P. Winkler, Localization of the motor hand area to a knob on the precentral gyrus. A new landmark. *Brain* **120** (Pt. 1), 141–157 (1997).
67. N. Kriegeskorte, M. Mur, P. Bandettini, Representational similarity analysis - connecting the branches of systems neuroscience. *Front. Syst. Neurosci.* **2**, 4 (2008).
68. N. M. Timme, C. Lapish, A tutorial for information theory in neuroscience. *eNeuro* **5**, ENEURO.0052-18.2018 (2018).
69. R. Alonso, I. Brocas, J. D. Carrillo, Resource allocation in the brain. *Rev. Econ. Stud.* **81**, 501–534 (2013).
70. V. Lee, J. Maguire, The impact of tonic $GABA_A$ receptor-mediated inhibition on neuronal excitability varies across brain region and cell type. *Front. Neural Circuits* **8**, 3 (2014).
71. G. H. Recanzone, M. M. Merzenich, W. M. Jenkins, K. A. Grajski, H. R. Dinse, Topographic reorganization of the hand representation in cortical area 3b owl monkeys trained in a frequency-discrimination task. *J. Neurophysiol.* **67**, 1031–1056 (1992).
72. C. Knight Fle, M. R. Longo, A. J. Bremner, Categorical perception of tactile distance. *Cognition* **131**, 254–262 (2014).
73. H. H. Schutt, S. Harmeling, J. H. Macke, F. A. Wichmann, Painfree and accurate Bayesian estimation of psychometric functions for (potentially) overdispersed data. *Vision Res.* **122**, 105–123 (2016).
74. L. M. Parsons, Imagined spatial transformations of one's hands and feet. *Cogn. Psychol.* **19**, 178–241 (1987).
75. D. N. Greve, B. Fischl, Accurate and robust brain image alignment using boundary-based registration. *Neuroimage* **48**, 63–72 (2009).
76. A. Hahamy, S. N. Macdonald, F. van den Heiligenberg, P. Kieliba, U. Emir, R. Malach, H. Johansen-Berg, P. Brugger, J. C. Culham, T. R. Makin, Representation of multiple body parts in the missing-hand territory of congenital one-handers. *Curr. Biol.* **27**, 1350–1355 (2017).
77. A. Hahamy, T. R. Makin, Remapping in cerebral and cerebellar cortices is not restricted by somatotopy. *J. Neurosci.* **39**, 9328–9342 (2019).
78. F. M. Z. van den Heiligenberg, T. Orlov, S. N. Macdonald, E. P. Duff, D. Henderson Slater, C. F. Beckmann, H. Johansen-Berg, J. C. Culham, T. R. Makin, Artificial limb representation in amputees. *Brain* **141**, 1422–1433 (2018).
79. S. B. Eickhoff, K. E. Stephan, H. Mohlberg, C. Grefkes, G. R. Fink, K. Amunts, K. Zilles, A new SPM toolbox for combining probabilistic cytoarchitectonic maps and functional imaging data. *Neuroimage* **25**, 1325–1335 (2005).
80. Y. Behzadi, K. Restom, J. Liau, T. T. Liu, A component based noise correction method (CompCor) for BOLD and perfusion based fMRI. *Neuroimage* **37**, 90–101 (2007).
81. S. Whitfield-Gabrieli, A. Nieto-Castanon, Conn: A functional connectivity toolbox for correlated and anticorrelated brain networks. *Brain Connect.* **2**, 125–141 (2012).
82. Y. Zhang, M. Brady, S. Smith, Segmentation of brain MR images through a hidden Markov random field model and the expectation-maximization algorithm. *IEEE Trans. Med. Imaging* **20**, 45–57 (2001).

Acknowledgments: We thank D. Stirling, S. Cousins, L. Mardell, M. Kromm, and M. Kollamkulam for help with data collection; E. Tupitsyna for developing the script for the kinematic data analysis; J. Kilner for providing us access to the CyberGlove; J. Diedrichsen for the custom-made force keyboards; H. Bowman for introducing us to information theory measures; G. Salvietti for invaluable technical help during piloting; S. Micera, J. Alvaro Gallego, and D. Wesselink for helpful comments on the manuscript; H. Schone for proofreading the manuscript; D. Prattichizzo for inspiring discussions about supernumerary fingers; and our participants for taking part in this study. **Funding**: This work was supported by an ERC Starting Grant (715022 EmbodiedTech), awarded to T.R.M., who was further funded by a Wellcome Trust Senior Research Fellowship (215575/Z/19/Z) and by Sir Halley Stewart Charitable Trust (580). **Author contributions:** P.K., R.O.M.-M., and T.R.M. conceived and designed the study. D.C. designed the Third Thumb. P.K. and D.C. performed the experiments. P.K. and R.O.M.-M. analyzed the data. P.K. and T.R.M. wrote the manuscript with input from all coauthors. **Competing interests:** D.C. is a sole trader at Dani Clode designs. The other authors declare that they have no competing interests. **Data and materials availability**: The data that support the findings of this study will be available from the Open Science Framework upon publication (https://osf.io/qgy8a/).

Submitted 13 July 2020
Accepted 23 April 2021
Published 19 May 2021
10.1126/scirobotics.abd7935

Citation: P. Kieliba, D. Clode, R. O. Maimon-Mor, T. R. Makin, Robotic hand augmentation drives changes in neural body representation. *Sci. Robot.* **6**, eabd7935 (2021).

Science Robotics

Robotic hand augmentation drives changes in neural body representation

Paulina Kieliba, Danielle Clode, Roni O. Maimon-Mor, and Tamar R. Makin

Sci. Robot. **6** (54), eabd7935. DOI: 10.1126/scirobotics.abd7935

Science Robotics (ISSN 2470-9476) is published by the American Association for the Advancement of Science. 1200 New York Avenue NW, Washington, DC 20005. The title *Science Robotics* is a registered trademark of AAAS.